



## Biosorption of Pb(II) from water using biomass of *Aeromonas hydrophila*: Central composite design for optimization of process variables

S.H. Hasan<sup>a,\*</sup>, P. Srivastava<sup>a</sup>, M. Talat<sup>b</sup>

<sup>a</sup> Water Pollution Research Laboratory, Department of Applied Chemistry, Institute of Technology, Banaras Hindu University, Varanasi 221 005, India

<sup>b</sup> Department of Biochemistry, Faculty of Science, Banaras Hindu University, Varanasi 221005, India

### ARTICLE INFO

#### Article history:

Received 29 December 2008

Received in revised form 26 February 2009

Accepted 26 February 2009

Available online 13 March 2009

#### Keywords:

*Aeromonas hydrophila*

Pb(II)

Biosorption mechanism

Optimization

Response surface methodology

Isotherm

### ABSTRACT

Biomass of *Aeromonas hydrophila* was successfully utilized for the removal of lead from aqueous solution. The effect of process variables such as pH, initial Pb(II) concentration, biomass dose and temperature on the uptake of lead were investigated using two level four factor ( $2^4$ ) full factorial central composite design with the help of MINITAB<sup>®</sup> version 15 software. The predicted results thus obtained were found to be in good agreement ( $R^2 = 98.6\%$ ) with the results obtained by performing experiments. The multiple regression analysis and analysis of variance (ANOVA) showed that the concentration has positive and temperature and biomass dose have negative whereas pH has curved relationship with the uptake of Pb(II). The maximum uptake of Pb(II) predicted by optimization plots was 122.18 mg/g at 20 °C, initial Pb(II) concentration of 259 mg/L, pH 5.0, temperature 20 °C and biomass dose 1.0 g. Langmuir isotherm model was applicable to sorption data and sorption capacity was found to be 163.3 mg/g at 30 °C, pH 5.0 and Pb(II) concentration range 51.8–259 mg/L indicate that the biosorbent was better in comparison of the biosorbent reported in the literature. Dubinin–Radushkevich (D–R) isotherm model was also applied and it was found that sorption was chemisorption ( $E = 12.98$  kJ/mol). FT-IR studies indicate the involvement of various functional groups present on biomass surface in the sorption of Pb(II).

© 2009 Elsevier B.V. All rights reserved.

### 1. Introduction

The presence of heavy metals in the environment specifically in various water resources is of major concern because of their toxicity, non-biodegradable nature and threat to human, animal and plant life. The major sources of water contamination are mining activities, agricultural run off, and industrial and domestic effluents [1]. Among various metal ions present in wastewater Pb(II) is one of the most prevalent metals. Pb has been introduced into natural water from a variety of sources such as storage batteries, lead smelting, tetraethyl lead manufacturing, mining, plating, ammunition, and the ceramic glass industries [2]. The major biochemical effects of Pb(II) are its interference with heme synthesis, plumbism, change in brain wave (EEG) patterns, protoporphyrin elevation in RBCs, interference with neurotransmission, impairment of vitamin D activity, blue lead line in gums, bone marrow damage, paralysis of wrist joints, degeneration of offspring, sterility, encephalopathy conditions, disturbance in cerebral function, dyspepsia, vertigo and kidney damage [3]. It is therefore, essential to remove Pb(II) from wastewater before disposal.

Conventional techniques for removing Pb(II) ions from aqueous system include ion exchange, filtration, chemical treatment, solvent extraction, membrane technology, precipitation and reverse osmosis. However, these processes have technical and/or economical constraints [4]. In this context, biosorption has emerged as an alternative to these traditional methods with the advantage of being technically easy, potential for regeneration and sludge free operation. In addition to this, it is ecofriendly in nature, has excellent performance, and is a low cost domestic technique for remediating even heavily metal loaded water [5,6]. Various biosorbents such as agricultural byproducts and microorganisms have been reported for efficiently accumulating heavy metals [7–17]. Among microorganisms, bacterial biomass (both live and dead) have gained attention of researchers for the removal of metal from aqueous solution during recent years because of their ubiquity and smaller size, which leads to high surface area and fast rates [7,18]. Nevertheless several functional groups such as carboxyl, amine, and hydroxyl groups are reported to be present as bacterial cell wall component due to which bacteria are capable of sorbing metal ions from aqueous solution. Aeromonads (a bacterial strain) have been reported for remediation of metal because they are ubiquitous in fresh and marine water and tolerant toward heavy metals [19]. In this series, *Aeromonas caviae* has already been used for the removal of Cr(VI) and Cd(II) [20,21] and *Aeromonas hydrophila* has also been used for the removal of Cr(VI) in our laboratory [22]. The present investigation is primarily

\* Corresponding author. Tel.: +91 542 25755758/9839089919 (Mobile).

E-mail addresses: [shhasan.apc@itbhu.ac.in](mailto:shhasan.apc@itbhu.ac.in), [hasanitbhu@yahoo.co.in](mailto:hasanitbhu@yahoo.co.in) (S.H. Hasan).

aimed to test the potential of biomass of *A. hydrophila* for the sorption of lead from water and to optimize the parameters affecting the sorption for its maximum removal via a  $2^4$  full factorial central composite response surface methodology (RSM) experimental design with the help of software MINITAB® version 15 software [23]. In the conventional method, there is a variation of only one parameter at a time, keeping the other parameters constant, and thus, the cumulative effect of all the affecting parameters at a time cannot be studied. This method is also time consuming and requires a number of experiments to be performed to determine the optimum levels, which is unreliable [24,25]. However, in RSM, the interactions of two or more variables can be studied simultaneously. In addition to this, it results in higher percentage yields, reduced process variability, closer confirmation of the output response to nominal and target achievement, and less treatment time with minimum costs [26].

## 2. Materials and methods

### 2.1. Stock solution

All chemicals and reagents used for experiments and analyses were of analytical grades. Stock solutions of 1000 mg/L Pb(II) were prepared from  $\text{Pb}(\text{NO}_3)_2$  in deionized, doubled distilled water containing a few drops of concentrated  $\text{HNO}_3$  to prevent hydrolysis of Pb(II).

### 2.2. Preparation of biosorbent

The strain used in this study was *A. hydrophila* (MTCC 646), a pure culture obtained from the Microbial Type Culture Collection & Gene Bank, Institute of Microbial Technology, Chandigarh, India. The culture was routinely maintained at 4 °C on nutrient agar medium slant and aerobically cultivated in nutrient broth containing: beef extract 10 g/L, NaCl 5 g/L and peptone 20 g/L. The initial pH of the culture was adjusted to 7.0–7.5. The flasks were incubated at 30 °C in a rotatory shaker agitated at 200 rpm for 24 h. The growing cells from the culture broth were separated from the liquid by centrifugation at 5000 rpm for 5 min and washed with deionized water. The wet cell biomass was dried for 24 h at 60 °C in an oven. Dried cells were powdered by blender in uniform size (100  $\mu\text{m}$ ) and used for experiment.

### 2.3. Biosorption studies

Batch experiments were carried out in Erlenmeyer flasks by adding dried cells of *A. hydrophila* in 50 mL of aqueous lead solution of desired initial concentration. The pH of the solution was initially adjusted by adding 0.1 M HCl and 0.1 M NaOH solution. The flasks were gently agitated in an electrically thermo stated reciprocating shaker at 200 rpm for a period of 80 min. The content of flask was separated from biosorbent by centrifuging at 15,000 rpm and was analyzed for remaining Pb(II) concentration in the sample. The amount of Pb(II) sorbed per unit mass of the biosorbent ( $q$  in mg/g) was evaluated by using following equations;

$$q(\text{mg/g}) = (C_i - C_e) \frac{V}{M} \quad (1)$$

where  $C_i$  and  $C_e$  are the Pb(II) concentrations in mg/L initially and at a given time  $t$ , respectively;  $V$  is the volume of the Pb(II) solutions in mL;  $M$  is the weight of biosorbent in g. Experiments were conducted in triplicate and the concurrent values were taken as result.

**Table 1**

Central composite design analysis for biosorption of Pb(II).

Independent variable		Range				
		$-\alpha$	-1	0	1	$\alpha$
Concentration (mg/L)	$X_1$	51.8	103.6	155.4	207.2	259
pH	$X_2$	4.0	4.5	5.0	5.5	6.0
Temperature (°C)	$X_3$	20	30	40	50	60
Biomass dose (g)	$X_4$	1.0	1.5	2.0	2.5	3.0

### 2.4. Analysis of Pb(II) in aqueous solution

A Shimadzu AA-6300 (Japan) atomic absorption spectrophotometer was used as detector with hollow cathode lamp light source set at 283.3 nm wavelength, using 10 mA lamp current and 0.7 nm slit width, and with deuterium lamp for background correction. Instrument grade (98%) acetylene, delivered at 4.0 L/min at a pressure of 0.9 kg/cm<sup>2</sup>, was used to generate the flame for the AAS together with compressed air supplied at 17.5 L/min flow rate and 3.5 kg/cm<sup>2</sup> gas pressure. The instrument was calibrated from 0.1 to 10.0 mg/L. Other range samples were diluted until results within the calibration range were obtained.

### 2.5. Infrared spectroscopy (IR) study

The samples of biosorbents (free and metal treated) were dried overnight to remove any water retained which could interfere with observation of hydroxyl groups on the surface. This was followed by encapsulation into dry potassium bromide (KBr) discs. The discs were then scanned into transmission mode using a Fourier transform infrared (FT-IR) spectrometer (Perkin Elmer Model No. 171097), through a wavelength range from 400 to 4000 cm<sup>-1</sup>. IR spectra of control and metal treated biomass were recorded.

## 3. Results and discussion

### 3.1. Optimization of biosorption process using RSM approach

The range of variables affecting the sorption of Pb(II) (i.e., pH, initial metal ion concentration, biomass dose, and temperature) as per CCD design is represented in Table 1. Since in the present investigation there are four variables, 31 experimental runs were required as per  $2^4$  full factorial designs (Table 2). Experiments were performed according to the above experimental plan, and the results are given in Table 3 along with the results predicted by the model with the help of MINITAB® version 15 software's. Significant changes in uptake of Pb(II) were observed for all the combinations, implying that all the variables were significantly affecting the sorption of Pb(II).

#### 3.1.1. Interpretation of the regression analysis

The response surface regression results thus obtained from CCD namely  $T$  and  $P$  values along with the constant and coefficients (estimated using coded values) are given in Table 4. The  $T$ -value is used

**Table 2**

Number of experimental runs required and their details for  $2^4$  full factorial central composite design.

Central composite design					
Factors	Replicates	Base runs	Total runs	Base blocks	Total blocks
4	1	31	31	1	1
Two-level factorial: full factorial					
Cube points	Center points in cube	Axial points	Center points in axial	Alpha	
16	7	8	0	2	

**Table 3**

Full factorial central composite design matrix of four variables (factors) along with experimental and predicted response (uptake) (mg/g).

Std. order	Run order	Pt type	Blocks	Concentration (mg/L)	pH	Temperature (°C)	Biomass dose (g)	Exp. uptake (mg/g)	Predicted (mg/g)	Residual
26	1	0	1	155.4	5.0	40	2.0	45.65	45.38	0.270
6	2	1	1	103.6	4.5	30	1.5	56.50	52.69	3.810
25	3	0	1	207.2	5.5	50	2.5	33.18	34.66	-1.480
2	4	1	1	155.4	6.0	40	2.0	28.81	28.53	0.280
20	5	-1	1	103.6	5.5	30	1.5	30.18	35.57	-5.390
17	6	-1	1	103.6	5.5	50	2.5	20.30	19.31	0.990
7	7	1	1	155.4	5.0	20	2.0	48.60	45.16	3.430
13	8	1	1	155.4	5.0	60	2.0	27.90	30.15	-2.250
28	9	0	1	155.4	5.0	40	2.0	45.65	45.38	0.270
16	10	1	1	155.4	5.0	40	2.0	45.65	45.38	0.270
4	11	1	1	207.2	5.5	50	1.0	93.98	92.70	1.280
22	12	-1	1	207.2	5.5	30	1.5	71.58	71.58	0.000
12	13	1	1	155.4	5.0	40	2.0	45.65	45.38	0.270
23	14	-1	1	103.6	4.5	50	2.5	24.30	22.61	1.689
21	15	-1	1	207.2	4.5	30	1.5	75.16	79.01	-3.851
8	16	1	1	103.6	4.5	50	1.5	40.31	44.15	-3.847
5	17	1	1	155.4	5.0	40	1.0	85.92	84.38	1.531
14	18	1	1	207.2	4.5	50	2.5	30.81	28.27	2.540
27	19	0	1	155.4	4.0	40	2.0	39.27	39.25	0.013
9	20	1	1	103.6	5.5	50	1.5	40.31	40.43	-0.120
30	21	0	1	51.8	5.5	40	2.0	15.98	12.42	3.552
29	22	0	1	207.2	5.5	30	2.5	43.90	41.14	2.758
18	23	-1	1	155.4	5.0	40	3.0	31.10	32.40	-1.30
19	24	-1	1	155.4	5.0	40	2.0	45.65	45.38	0.27
10	25	1	1	103.6	5.5	30	2.5	13.80	16.21	-2.41
24	26	-1	1	103.6	4.5	30	2.5	29.90	32.89	-2.99
15	27	1	1	155.4	5.0	40	2.0	45.65	45.38	0.270
31	28	0	1	207.2	4.5	30	2.5	48.18	48.14	0.040
3	29	1	1	207.2	4.5	50	1.5	63.21	60.89	2.320
1	30	1	1	259.0	5.0	40	2.0	62.13	64.50	-2.372
11	31	1	1	155.4	5.0	40	2.0	45.65	45.38	0.270

to determine the significance of the regression coefficients of the parameters and the  $P$ -value is defined as the smallest level of significance leading to rejection of null hypothesis. In general, the larger the magnitude of  $T$  and smaller the value of  $P$ , the more significant is the corresponding coefficient term [24].

The value of constant was found to be 45.3871 and was significant because the values of  $T$  and  $P$  were 39.306 and 0.000 respectively. The value of constant does not depend on any variable and interaction of the variables. This indicates that the average uptake of lead was 45.3871 mg/g and is independent of the experimental variables. The effect of all the linear terms such as concentration, pH, temperature and biomass dose were found to be highly significant because  $P$  values were less than 0.05. Thus there was a linear relation of all these parameters with the uptake of Pb(II). Like wise the effect of quadratic term of concentration, pH

and biomass dose were evaluated and it has been found that the quadratic terms of pH ( $P=0.000$ ) was more significant in comparison to the linear terms of pH ( $P=0.001$ ). This indicate that pH has a curvature (quadratic response) with the uptake of Pb(II) that is why initially with increase of pH uptake will increase and after a maximum uptake, it will start decreasing with increase of pH. All the interaction terms except pH and biomass dose ( $P=0.888$ ) and temperature and biomass dose ( $P=0.565$ ) were also found significant. In addition to this, a positive sign of the coefficient represents a synergistic effect whereas a negative sign indicates an antagonistic effect. It has been found that the linear variables pH, biomass dose and temperature and the quadratic terms of pH, temperature and interactions term concentration and temperature, concentration and biomass dose have an antagonistic relationship with the biosorption process. That means with the increase of these factors the uptake of Pb(II) decrease. Whereas linear terms concentration and interaction term concentration and pH, pH and temperature and pH and biomass have a synergistic effect on the sorption of Pb(II). Thus with the increase of these variables the uptake of Pb(II) will increase. Finally, a regression equation was prepared using the values of coefficients, which is as follows:

$$\begin{aligned}
 Y = & 45.3871 + (+20.8376 * X_1) + (-5.3634 * X_2) + (-7.5043 * X_3) \\
 & + (-25.9932 * X_4) + (-1.7226 * X_1 * X_1) + (-11.4927 * X_2 * X_2) \\
 & + (-7.7266 * X_3 * X_3) + (+13.0097 * X_4 * X_4) \\
 & + (+9.6863 * X_1 * X_2) + (-9.5830 * X_1 * X_3) \\
 & + (-11.0695 * X_1 * X_4) + (+13.3920 * X_2 * X_3) \\
 & + (+0.4255 * X_2 * X_4) + (-1.7495 * X_3 * X_4) \quad (2)
 \end{aligned}$$

where  $Y$  is the predicted value of sorption of Pb(II) in mg/g and  $X_1$ ,  $X_2$ ,  $X_3$ ,  $X_4$  are concentration of Pb(II), pH, temperature and biomass dose respectively. The low value of standard deviation

**Table 4**

Estimated regression coefficients for experimental uptake (mg/g).

Term	Coefficient	Standard error coefficient	$T$ -value	$P$ -value
Constant	45.3871	1.161	39.106	0.000
$X_1$	20.8376	1.305	15.964	0.000
$X_2$	-5.3634	1.267	-4.234	0.001
$X_3$	-7.5043	1.278	-5.873	0.000
$X_4$	-25.9932	1.234	-21.058	0.000
$X_1 * X_1$	-1.7226	2.405	-0.716	0.484
$X_2 * X_2$	-11.492	2.351	-4.888	0.000
$X_3 * X_3$	-7.7266	2.330	-3.316	0.004
$X_4 * X_4$	13.0097	2.199	5.915	0.000
$X_1 * X_2$	9.6863	2.994	3.235	0.005
$X_1 * X_3$	-9.5830	3.139	-3.053	0.008
$X_1 * X_4$	-11.0695	2.979	-3.716	0.002
$X_2 * X_3$	13.3920	3.139	4.266	0.001
$X_2 * X_4$	0.4255	2.979	0.143	0.888
$X_3 * X_4$	-1.7495	2.979	-0.587	0.565

$S = 3.110$ ;  $R\text{-Sq} = 98.6\%$ ;  $R\text{-Sq (adj)} = 97.3\%$ .

**Table 5**  
Analysis of variance (ANOVA) for Pb(II) uptake (mg/g).

Source	Degree of freedom	Sum of square (SS)	Adj sum of square	Adj mean of square	F-value	P-value
Regression	14	10773.7	10773.73	769.55	79.55	0.000
Linear	4	9258.2	7428.12	1857.03	191.97	0.000
Square	4	993.8	738.91	184.73	19.10	0.000
Interaction	6	521.8	521.78	86.96	8.99	0.000
Residual error	16	154.8	154.78	9.67		
Lack-of-fit	10	154.8	154.78	15.48		
Pure error	6	0.0	0.00	0.00		
Total	30	10928.5				

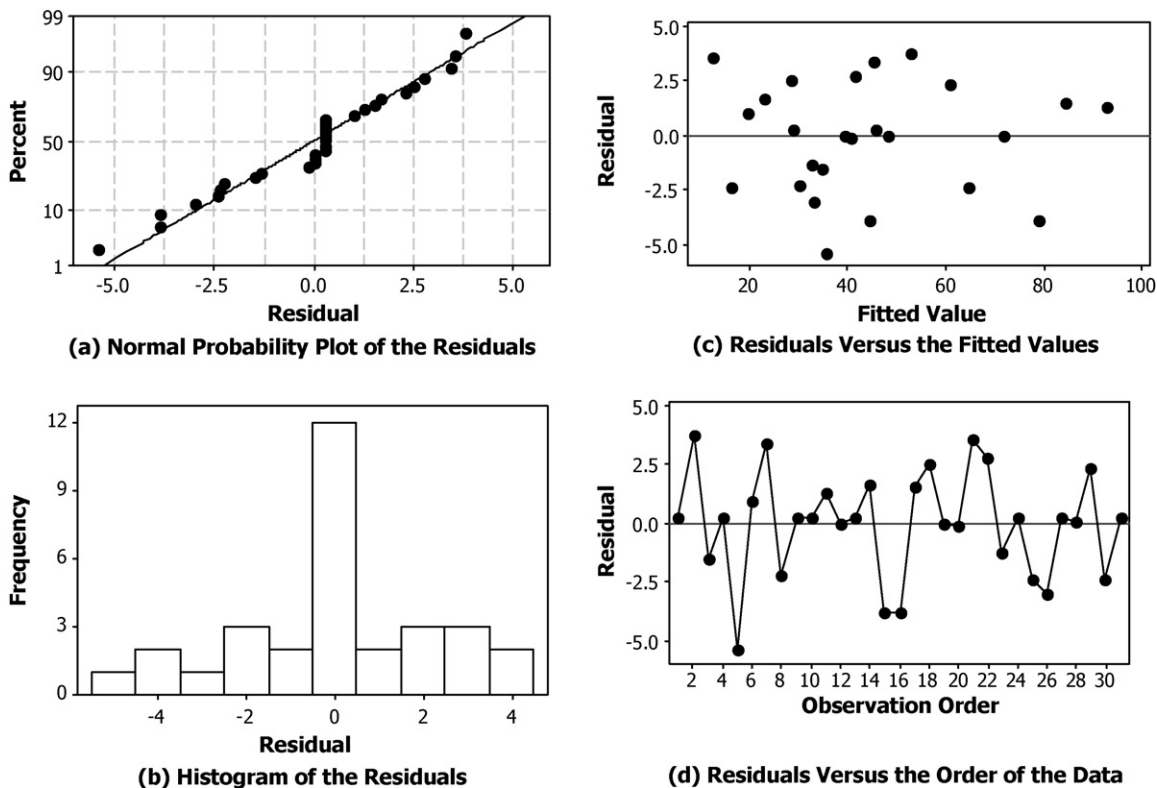


Fig. 1. Residual graphs (a) normal probability plot for residuals, (b) histograms of residuals, (c) residuals vs. fitted values and (d) residuals vs. the order of the data.

(3.111) between the experimental and predicted results shows that Eq. (2) adequately represents actual relationship between the response and significant variables. High value of  $R^2$  (98.6%) and  $R^2$  (adjusted) (97.3%) indicates a high dependence and correlation between the observed and the predicted values of response. The predicted values were found to be very close to the experimental results (Table 3).

The statistical significance of the ratio of mean square variation due to regression and mean square residual error was tested using analysis of variance (ANOVA). ANOVA is a statistical technique that subdivides the total variation in a set of data into component parts associated with specific sources of variation for testing hypothesis on the parameters of the model [27]. According to Table 5 the  $F_{Statistics}$  values for all regression were higher (79.55). The large value of  $F$  indicates that most of the variation in the response can be explained by the regression equation. The associated  $P$ -value is used to estimate whether  $F_{Statistics}$  is large enough to indicate statistically significant [28]. If  $P$ -value is lower than 0.05, and then it indicates that the model is statistically significant [29]. It was observed from ANOVA study that the coefficients for the linear ( $P=0.000$ ) and interaction ( $P=0.000$ ) effects were highly significant and thus confirm the applicability of the predicted model.

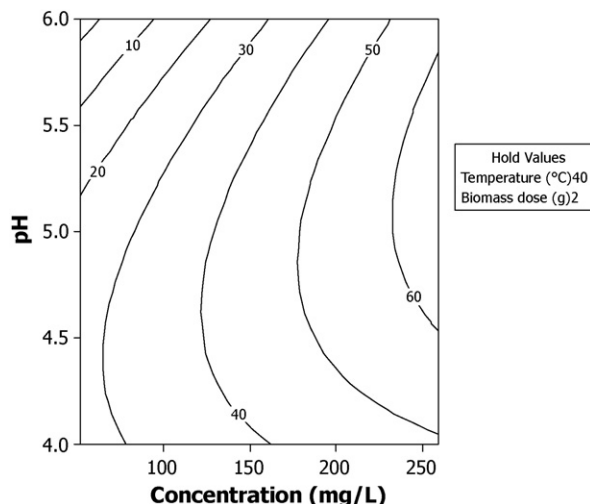


Fig. 2. Contour plot for uptake (mg/g) vs. pH and concentration.

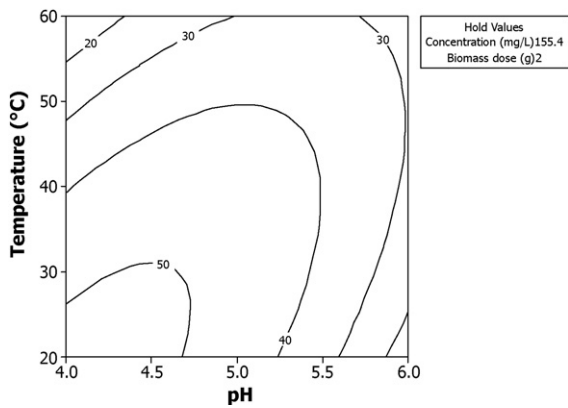


Fig. 3. Contour plot for uptake (mg/g) vs. pH and temperature.

### 3.1.2. Interpretation of residual graphs

The normality of the data can be checked by plotting the normal probability plot (NPP) of the residuals. The normal probability plot is a graphical technique for assessing whether or not a data set is approximately normally distributed [30]. The residual is the difference between the observed and the predicted value (or the fitted value) from the regression. If the points on the plot fall fairly close to the straight line then the data are normally distributed. Fig. 1(a) shows normal probability plot of residual values. It could be seen that the experimental points were reasonably aligned suggesting normal distribution. The results can be shown in Fig. 1(b) with the help of a histogram. Histograms of the residuals show the distribution of the residuals for all observations. The figure shows an almost symmetrical histogram (bell shaped i.e. the errors are normally distributed with mean zero) (Minitab® 15). Fig. 1(c) plots the residuals versus the fitted values (predicted response). The residuals are scattered randomly about zero i.e. the errors have a constant variance. Fig. 1(d) plots the residuals in the order of the corresponding observations. The residuals appear to be randomly scattered about zero and all other points were found to fall in the range of +5 to –5 except point –5.

### 3.1.3. Interpretation of contour plots

Contour plot is the projection of the response surface as a two-dimensional plane. This analysis gives a better understanding of the influence of variables and their interaction on the response. To investigate the interactive effect of two factors on the uptake of lead, the response surface methodology–central composite design was used, and contour plots were drawn. The hold values of the remaining factors were set at their middle values (i.e., pH at 5.0, initial metal ion concentration at 155.4 mg/L, temperature at 40 °C, and biomass dose at 2.0 g). Fig. 2 shows the combined effect of pH and initial metal ion concentration. It is clear from the figure that the uptake was increased with the increase in pH up to 5.0 then decreases and uptake increased with an increase in initial metal ion concentration. The maximum uptake was achieved at pH 5.0 and concentration of 259 mg/L. At solution pH lower than 4, the uptake capacity was lower due to competition between hydrogen and metal ions on the binding sites of biosorbent [31]. The maximum Pb(II) ions uptake onto *A. hydrophila* was observed at pH 5.0. As the solution pH increased more than pH 5.0, which resulted in precipitation of Pb(II) ions thus lower the biosorption efficiency [32]. The uptake of lead was found to increase as the initial metal ion concentration increased because the number of ions adsorbed from solutions of higher concentrations is more than that removed from less concentrated solutions. Fig. 3 shows the combined effect of pH and temperature on the uptake of lead. It reveals that the uptake was decreased with increase in temperature and increased

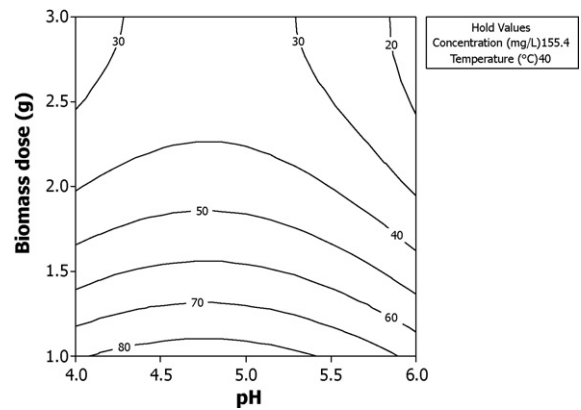


Fig. 4. Contour plot for uptake (mg/g) vs. pH and biomass dose.

with increase in pH up to 5.0, which was found to be in accordance with the experimental and predicted model values. The maximum uptake was found at temperature of 20 °C and pH 5.0. The increase in uptake with decreasing temperature could be explained because the decrease of temperatures favors the sorbate transport with in the pores of sorbent. Combined effect of pH and biomass dose was analyzed and presented in Fig. 4, showing that the uptake was decreased with the increase biomass dose and increased with increase in pH up to 5.0. The maximum uptake of Pb(II) was found at a biomass of 1.0 g and pH 5.0. The decrease in the uptake of Pb(II) with increasing sorbent dose was due to split in the flux or the concentration gradient between Pb(II) concentration in the solution and the Pb(II) concentration on the surface of the biosorbent, which finally reduces the uptake of Pb(II) onto the unit weight of sorbent.

### 3.1.4. Interpretation of process optimization curve

Response optimization helps to identify the factor settings that optimize a single response or a set of responses. It is useful in determining the operating conditions that will result in a desirable response. In the present study, the goal for Pb(II) uptake using biomass of *A. hydrophila* was to obtain a value at or near the target value of 125.0 mg/g. Uptake values less than 10 and greater than 150 mg/g were unacceptable. Both weight and importance were set at 1. The global solution, which is defined as the best combination of factor settings for achieving the desired response, was found to be pH 5.0, initial metal ion concentration 259 mg/L, temperature 20 °C and biomass dose 1.0 g for a predicted response of 122.18 mg/g with a desirability score of 0.9755 (Fig. 5). Thus a maximum uptake of Pb(II) of 122.18 mg/g can be achieved with *A. hydrophila* under the studied conditions. Other desired values can also be predicted by changing the current factor level setting in the optimization plot and then these values can be achieved by performing experiments. In general, there are many advantages of optimization plot to achieve predicted response with higher desirability score, lower

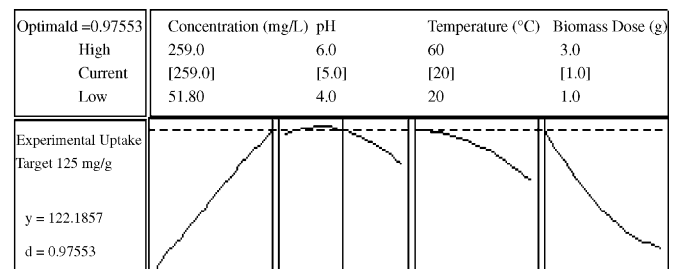


Fig. 5. Process optimization curve for a target value of 125 mg/g of Pb(II).

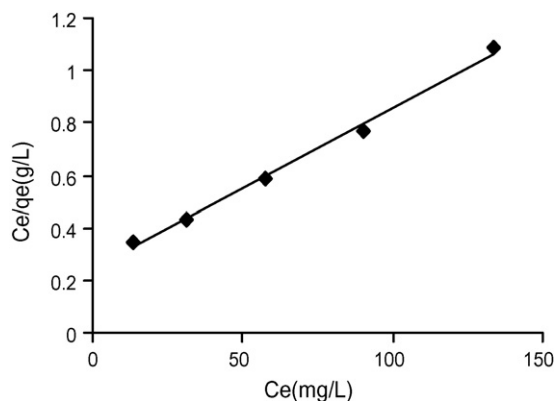


Fig. 6. Langmuir sorption isotherm plot.

cost factor settings with near optimal properties, to study the sensitivity of response variables to changes in the factor settings and to get required responses for factor settings of interest.

### 3.2. Adsorption equilibrium study

Various isotherm models have been utilized for describing sorption equilibrium for wastewater treatment. For the present work Langmuir and Dubinin–Radushkevich equations was being used to evaluate the sorption capacity of the biomass and the nature of sorption of lead on the surface of the biomass respectively. The study of isotherm was carried out by varying initial metal ion concentration from 51.8 to 259 mg/L at 30 °C temperature and pH 5.0.

#### 3.2.1. Langmuir sorption isotherm

The Langmuir sorption isotherm describes that the uptake occurs on a homogeneous surface by monolayer sorption without interaction between sorbed molecules [33]. The linear form of the Langmuir isotherms may be represented as:

$$\frac{C_e}{q_e} = \frac{1}{Q^0 b} + \frac{C_e}{Q^0} \quad (3)$$

where  $Q^0$  and  $b$  are the Langmuir constants related to the monolayer sorption capacity (mg/g) and free sorption energy (L/mg), respectively. The isotherm constants  $Q^0$  and  $b$  are calculated from the slope and intercept of plot between  $C_e/q_e$  and  $C_e$  (Fig. 6), respectively. The isotherm showed good fit to the experimental data with good correlation coefficients (0.996). The sorption capacity of the biomass of *A. hydrophila* was found to be 163.6 mg/g at 30 °C and pH 5.0, which

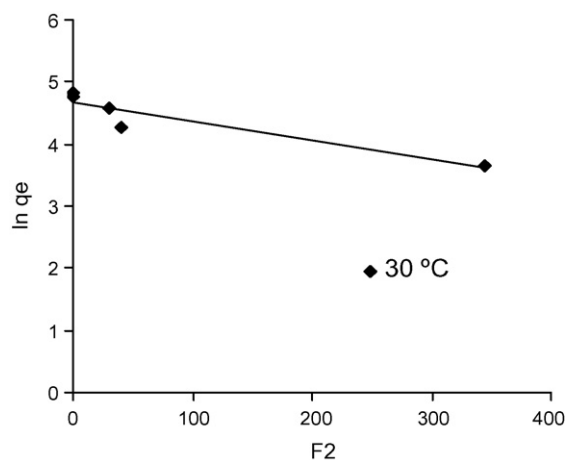


Fig. 7. Dubinin–Radushkevich isotherm plot.

is found to be much better than other biosorbents already used for the removal of lead from water (Table 6).

#### 3.2.2. Dubinin–Radushkevich (D–R) sorption isotherm

The data were also applied to Dubinin–Radushkevich (D–R) isotherm. This model envisages about the heterogeneity of the surface energies [34] and can be written in the following linear form:

$$\ln q_e = \ln X_m - BF^2 \quad (4)$$

$$F = RT \ln \left( 1 + \frac{1}{C_e} \right) \quad (5)$$

where  $q_e$  is the amount of sorbate sorbed by sorbent (mol/g),  $X_m$  is the maximum sorption capacity of the sorbent (mol/g),  $B$  is the constant related to energy (mol<sup>2</sup>/kJ<sup>2</sup>),  $F$  is the polar potential,  $R$  is the universal gas constant [8.314 J/(mol K)],  $T$  is the absolute temperature (Kelvin), and  $C_e$  the concentrations at equilibrium (mol/L).

The constants  $B$  and  $X_m$  were obtained from slope and intercept of the plot of  $\ln q_e$  against  $F^2$  (Fig. 7), respectively, and the values are  $-0.0030$  kJ<sup>2</sup>/mol<sup>2</sup> and 1.013 mol/g respectively. Thus, mean sorption energy,  $E$ , which is defined as the free energy transfer of 1 mol of solute from infinity of the surface of the sorbent, can be calculated using the calculated value of  $B$  from:

$$E = \frac{1}{\sqrt{-2B}} \quad (6)$$

If the magnitude of  $E$  is between 8 and 16 kJ/mol, the sorption process is supposed to proceed via chemisorption, while for values of  $E < 8$  kJ/mol, the sorption process is of physical nature.

Table 6

Comparison of sorption capacities of the *A. hydrophila* for the removal of Pb(II) with those of other biosorbents [7–15].

S. no. adsorbent	Operating conditions				Sorption capacity (mg/g)
	pH	Temperature (°C)	Concentration range (mg/L)	Biomass dose (g/L)	
1. <i>Saccharomyces cerevisiae</i>	5.0	25	10.4	2	2.7
2. <i>Pinus sylvestris</i>	4.0	25	10–100	4	11.38
3. <i>Phanerochaete chrysosporium</i> (formaldehyde and alkali pretreated)	4.5	27	50.00	2	12.34
4. <i>Mucor rouxii</i>	5.0	–	10	–	17.13
5. <i>S. noursei</i>	6.1	30	2–207	3.5	36.50
6. <i>Pseudomonas putida</i>	5.5	25	–	–	56.20
7. <i>Rhizopus arrhizus</i>	5–7	–	10–600	3	85.60
8. <i>Bacillus</i> sp. (ATS-1)	3.0	–	25–250	2	92.27
9. <i>Streptomyces longwoodensis</i>	3.0	28	50–200	0.3	100.00
10. <i>Spirogyra neglecta</i>	5.0	25	–	1.0	116.10
11. <i>S. rimosus</i> (NaOH treated)	2–12	–	10–800	3	135.00
12. <i>Spirogyra</i> sp.	5.0	45	–	–	151.58
13. <i>Aeromonas hydrophila</i> (present study)	5.0	30	51.8–259	1.0	163.30

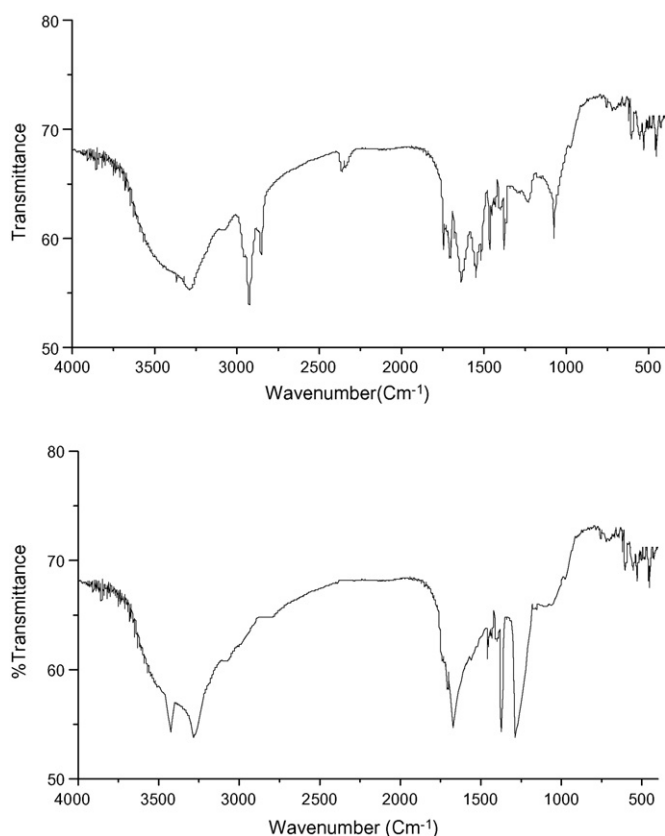


Fig. 8. (a) Free *Aeromonas hydrophila* and (b) Pb(II) loaded biomass.

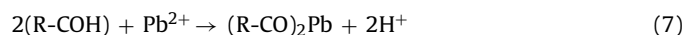
The isotherm showed good fit to the experimental data (Fig. 7) with good correlation coefficients (0.996). The applicability of this isotherm model to the lead sorption shows that there is possibility of heterogeneous energetic distribution of active sites on the surface of the sorbent. The estimated values of  $E$  for the present study were found 12.98 kJ/mol expected for chemical sorption. Thus, the sorption of Pb(II) on the surface of the *A. hydrophila* was chemisorption.

### 3.3. Biosorption mechanism

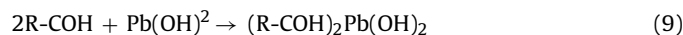
In order to interpret the sorption mechanism of Pb(II) ions on a sorbent surface, a knowledge of Pb(II) speciation and the sorbent surface characteristics is essential [35]. The major components of the polymeric material in *A. hydrophila* are carboxylic, phenolic and amines compounds which possess the capability of capturing heavy metal ions. It can be speculated that carboxylic or other compounds

are the active ion exchange sites. Based on the electron donating nature of the O-containing phenol and carboxyl groups in *A. hydrophila* and the electron-accepting nature of heavy metal ions, the ion exchange mechanism could be preferentially considered. For instance, a divalent heavy metal ion such as  $Pb^{2+}$  may attach itself to two adjacent hydroxyl groups which could donate two pair of electrons to the metal ion, forming four coordination number compounds and releasing two hydrogen ions into solution. It is then readily understood that the equilibrium is quite dependent on pH of the aqueous solution. At lower pH, the  $H^+$  ions compete with Pb(II) cations for the exchange sites on the *A. hydrophila*, thereby partially releasing the latter. The  $Pb^{2+}$  cations are completely released under circumstances of extreme acidic conditions. In most cases, the adsorbed amount of metal ions increased with an increase in pH up to a certain value and then decreased with further increase of pH. In a certain pH range for  $Pb^{2+}$ , there may be number of species present in solution, such as  $Pb^{2+}$ ,  $Pb(OH)^+$ ,  $Pb(OH)_2$ , etc. At lower pH, the positive charged lead ion species may compete with  $H^+$  and be adsorbed at the surface of the *A. hydrophila* by ion exchange mechanism. With an increase in pH, lead ion species, mainly neutral, may be adsorbed by hydrogen bonding mechanism along with ion exchange. These mechanisms are shown in the following equations [36–38].

Ion exchange



Hydrogen bonding



where  $R$  is the matrix of the *A. hydrophila*. The chemical bonding results from the sharing of a free electron pair between the surface oxygen atom and metal atom or the formation of an O–Pb(II) bond. An increase in pH shows an increase in adsorption up to 5 in which the surface of *A. hydrophila* is negatively charged and the sorbate species are also still positively charged. The increasing electrostatic attraction between positively charged sorbate species [ $Pb^{2+}$  and  $Pb(OH)^+$ ] and negative surface sites will lead to increased adsorption of Pb(II) on *A. hydrophila*.

### 3.4. Infrared spectroscopy study

In order to study the role of the functional groups present on the surface of biomass, FT-IR spectra of free and loaded biomass were taken (Fig. 8a and b). The FT-IR spectrum of the free biomass exhibit the presence of amino, carboxyl, and hydroxyl groups on the surface because of strong bands in the region 3500–3000  $cm^{-1}$  stretching of hydrogen bonded O–H, N–H of secondary amides and  $NH_3^-$  and

Table 7  
Infrared spectroscopic (FT-IR) study of free and Pb(II) loaded biomass of *A. hydrophila*.

Wavelength range ( $cm^{-1}$ )	Free cell ( $cm^{-1}$ )	Pb(II) laden cell ( $cm^{-1}$ )	Assignment
3500–3200	3368	3425, 3283	Bonded hydroxyl group ( $OH^-$ ) and primary and secondary amines and amides stretching (N–H stretching)
3000–2850	2920.10	–	C–H stretching
1750–1670	1745.5	1671.2	C=O stretching in carboxyl and amides groups (amide I band), C–N stretching in plane O–H bending and C–O stretching in ether
1640–1550	1639.64	–	Primary and secondary amines and amides stretching (N–H bending) and C=O stretching in carboxyl or amide groups (amide I band)
1550–1375	1379.23, 1464.10	–	Sulfamide bonds (S=O), symmetric and asymmetric bending of $CH_2$ and $CH_3$ groups respectively
1375–1300	–	1373.1	Amines, C–N Stretching in plane O–H bending
1350–1000	–	1287.23	C–O stretching of COOH
1300–1000	1074.5	–	Amines (C–N) stretching

those around 2920–2850  $\text{cm}^{-1}$  of alkyl chain. The stronger bands 1745.5  $\text{cm}^{-1}$  in the spectra of free biomass which were assigned to C=O stretching in carboxyl and amides groups (amide I band). The amide I band is primarily a C=O stretching mode and centered at 1639.64  $\text{cm}^{-1}$ . Sulfamide bonds (S=O), symmetric and asymmetric bending of  $\text{CH}_2$  and  $\text{CH}_3$  groups close to 1464.10 and 1379.23  $\text{cm}^{-1}$ . The strong band within 1100–1000  $\text{cm}^{-1}$  was due to C–O bond, which is characteristic peak for polysaccharide. 1074.5  $\text{cm}^{-1}$  peak shows the presence of amines (C–N) stretching.

Conspicuous changes (appearance and disappearance) in the FT-IR spectrum of loaded biomass have been found (Table 7). A shifting of 3368  $\text{cm}^{-1}$  into two new peaks 3425 and 3283  $\text{cm}^{-1}$  indicating the involvement of O–H bonding and N–H of secondary amides and  $\text{NH}_2^-$ . Further, the peak at 1745.5 shifted to 1671.2  $\text{cm}^{-1}$  indicating the involvement C=O stretching of carboxyl and amides groups (amide I band). A new peak at 1373.1 and 1287.23  $\text{cm}^{-1}$  appear which indicates that amines, C–N stretching in plane O–H bending and C–O stretching of COOH groups were also involved in lead biosorption.

#### 4. Conclusion

The following conclusion can be drawn from this study:

1. The biomass of *A. hydrophila* was found to be a potential biosorbent for the uptake of Pb(II) from water. A  $2^4$  full factorial central composite design was utilized with the help of MINITAB® 15 (trial version) software for predicting the results with 31 sets of experiments, and a high correlation has been found between the experimental and predicted values ( $R^2 = 98.6\%$ ).
2. The uptake of lead was found to be very sensitive to the linear effect of all the factors, viz., pH, metal ion concentration, temperature, and biomass dose. The uptake was found to increase with an increase in Pb(II) concentration and decrease with the biomass dose and temperature whereas in the case of pH the uptake initially increases with the increase of pH and after maximum uptake it started decreasing with increase of pH. In this study, the predicted maximum uptake of Pb(II), i.e., 122.1857 mg/g was obtained at initial metal ion concentration 259 mg/L, pH 5.0, temperature 20 °C, and biomass dose 1.0 g.
3. The sorption of Pb(II) on *A. hydrophila* was found to follow both Langmuir and D–R isotherm, suggesting the monolayer sorption as well as heterogeneous energetic distribution of active sites on the surface of the sorbent. The sorption capacity of biomass *A. hydrophila* was found 163.6 mg/g at 30 °C, pH 5.0 and concentration range 51.8–259 mg/L, and the process of sorption was chemisorption.
4. FT-IR study shows the involvement of carboxyl, hydroxyl and amine groups in the sorption of Pb(II).

#### Acknowledgments

The authors are thankful to Institute of Technology, Banaras Hindu University and University Grant Commission (UGC) (F. No. 32-224/2006 (SR)) for laboratory facilities and financial assistance.

#### References

- [1] V.K. Gupta, A. Rastogi, Biosorption of lead(II) from aqueous solutions by non-living algal biomass *Oedogonium* sp. and *Nostoc* sp.—a comparative study, *Colloids Surf. B* 64 (2008) 170–178.
- [2] V. Singh, S. Tiwari, A.K. Sharma, R. Sanghi, Removal of lead from aqueous solutions using *Cassia grandis* seed gum-graft-poly (methylmethacrylate), *J. Colloid Interface Sci.* 316 (2007) 224–232.
- [3] S.S. Dara, A Textbook of Environmental Chemistry and Pollution Control, S. Chand & Company LD, 2005, ISBN 81-219-083-3.
- [4] B. Volesky, Detoxification of metal bearing effluents: biosorption for the next century, *Hydrometallurgy* 59 (2001) 203–216.
- [5] R.H.S.F. Viera, B. Volesky, Biosorption: a solution to pollution? *Int. Microbiol.* 3 (2000) 17–24.
- [6] V.K. Gupta, A. Rastogi, Biosorption of lead from aqueous solutions by green algae *Spirogyra* species: kinetics and equilibrium studies, *J. Hazard. Mater.* 152 (2008) 407–414.
- [7] K. Vijayaraghavan, Y.S. Yun, Bacterial biosorbents and biosorption, *Biotechnol. Adv.* 26 (2008) 266–291.
- [8] A. Singh, D.J.P. Gaur, Copper(II) and lead(II) sorption from aqueous solution by non-living *Spirogyra neglecta*, *Bioresour. Technol.* 98 (2007) 3622–3629.
- [9] H. Uzun, Y.K. Bayhan, Y. Kaya, A. Cakici, O.F. Algur, Biosorption of lead(II) from aqueous solution by cone biomass of *Pinus sylvestris*, *Desalination* 154 (2003) 233–238.
- [10] G. Yan, T. Viraraghavan, Effect of pretreatment on the bioadsorption of heavy metals on *Mucor rouxii*, *Water SA* 26 (2000) 119–123.
- [11] B. Mattuschka, G. Straube, Biosorption of metals by a waste biomass, *J. Chem. Technol. Biotechnol.* 58 (1993) 57–63.
- [12] E. Fourest, J.C. Roux, Heavy metal biosorption by fungal mycelial byproducts: mechanism and influence of pH, *Appl. Microbiol. Biotechnol.* 37 (1992) 399–403.
- [13] Q. Li, S. Wu, G. Liu, X. Liao, X. Deng, D. Sun, Y. Hu, Y. Huang, Simultaneous biosorption of cadmium(II) and lead(II) ions by pretreated biomass of *Phanerochaete chrysosporium*, *Sep. Purif. Technol.* 34 (2004) 135–142.
- [14] N. Friis, P.M. Keith, Biosorption of uranium and lead by *Streptomyces longwoodensis*, *Biotechnol. Bioeng.* 28 (1986) 21–28.
- [15] C.P. Huang, C.P. Huang, A.L. Morehart, The removal of Cu(II) from dilute aqueous solution by *Saccharomyces cerevisiae*, *Water Res.* 24 (1990) 433–439.
- [16] K.K. Singh, M. Talat, S.H. Hasan, Removal of lead from aqueous solutions by agricultural waste maize bran, *Bioresour. Technol.* 97 (2006) 2124–2130.
- [17] S.H. Hasan, K.K. Singh, O. Prakash, M. Talat, Y.S. Ho, Removal of Cr(VI) from aqueous solutions using agricultural waste 'maize bran', *J. Hazard. Mater.* 152 (2008) 356–365.
- [18] D. Mohan, C.U. Pittman Jr., Activated carbons and low cost adsorbents for remediations of tri- and hexavalent chromium from water, *J. Hazard. Mater.* 137 (B) (2006) 762–811.
- [19] C.D. Miranda, G. Castillo, Resistance to antibiotic and heavy metals of motile aeromonads from Chilean freshwater, *Sci. Total Environ.* 224 (1998) 167–176.
- [20] M.X. Loukidou, T.D. Karapantsios, A.I. Zoubolis, K.A. Matis, Diffusion kinetic study of cadmium(II) biosorption by *Aeromonas caviae*, *J. Chem. Technol. Biotechnol.* 79 (2004 a) 711–719.
- [21] M.X. Loukidou, T.D. Karapantsios, A.I. Zoubolis, K.A. Matis, Diffusion kinetic study of chromium(VI) biosorption by *Aeromonas caviae*, *Ind. Eng. Chem. Res.* 43 (2004) 1748–1755.
- [22] D. Ranjan, P. Srivastava, M. Talat, S.H. Hasan, Biosorption of Cr(VI) from water using biomass of *Aeromonas hydrophila*: central composite design for optimization of process variables, *J. Appl. Biochem. Biotechnol.*, in press.
- [23] MINITAB® Release 15 Statistical Software for Windows, 2006, Minitab Inc., USA.
- [24] K. Ravikumar, S. Krishnan, S. Ramalingam, K. Balu, Application of response surface methodology to optimize process variable for reactive red and acid brown dye removal using a novel adsorbent, *Dyes Pigments* 72 (2007) 66–74.
- [25] I.A.W. Tan, A.L. Ahmad, B.H. Hameed, Optimization of preparation conditions for activated carbons from coconut husk using response surface methodology, *Chem. Eng. J.* 137 (2008) 462–470.
- [26] G.E.P. Box, J.S. Hunter, Multifactor experimental design for exploring response surfaces, *Ann. Math. Stat.* 28 (1957) 195–241.
- [27] J. Segurolo, N.S. Allen, M. Edge, A.M. Mahon, Design of eutectic photo initiator blends for UV/curable curable acrylated printing inks and coatings, *Prog. Org. Coat.* 37 (1999) 23–37.
- [28] H.M. Kim, J.G. Kim, J.D. Cho, J.W. Hong, Optimization and characterization of U.V.-curable adhesives for optical communication by response surface methodology, *Polym. Test* 22 (2003) 899–906.
- [29] M.M.D. Zulkali, A.L. Ahmad, N.H. Norulakmal, *Oryza sativa* L. husk as heavy metal adsorbent: optimization with lead as model solution, *Bioresour. Technol.* 97 (2006) 21–25.
- [30] D. Pokhrel, T. Viraraghavan, Arsenic removal from aqueous solution by iron oxide coated fungal biomass: a factorial design analysis, *Water Air Soil Pollut.* 173 (2006) 195–208.
- [31] A. Pavan Flávio, A.C. Mazzocato, A. Jacques Rosângela, L.P. Dias Silvio, Ponkan peel: a potential biosorbent for removal of Pb(II) ions from aqueous solution, *Biochem. Eng. J.* 40 (2008) 357–362.
- [32] G. Yan, T. Viraraghavan, Heavy-metal removal from aqueous solution by fungus *Mucor rouxii*, *Water Res.* 37 (2003) 4486–4496.
- [33] I. Langmuir, *J. Am. Chem. Soc.* 40 (1918) 1361–1368.
- [34] M.M. Dubinin, L.V. Radushkevich, Proceedings of the Academy of Sciences of the USSR, Chemistry Section 55, 1947, pp. 331–333.
- [35] K.A. Krishnan, A. Sheela, T.S. Anirudhan, Kinetic and equilibrium modeling of liquid-phase adsorption of lead and lead chelates on activated carbons, *J. Chem. Technol. Biotechnol.* 78 (2003) 642–653.
- [36] M. Ozacar, I.A.S. Engil, Adsorption of metal complex dyes from aqueous solutions by pine sawdust, *Bioresour. Technol.* 96 (2005) 791–795.
- [37] A. Shukla, Y.H. Zhang, P. Dubey, J.L. Margrave, S.S. Shukla, The role of sawdust in the removal of unwanted materials from water, *J. Hazard. Mater.* B95 (2002) 137–152.
- [38] A. Ornek, M. Ozacar, I.A. Şengil, Adsorption of lead onto formaldehyde or sulphuric acid treated acorn waste: equilibrium and kinetic studies, *Biochem. Eng. J.* 37 (2007) 192–200.